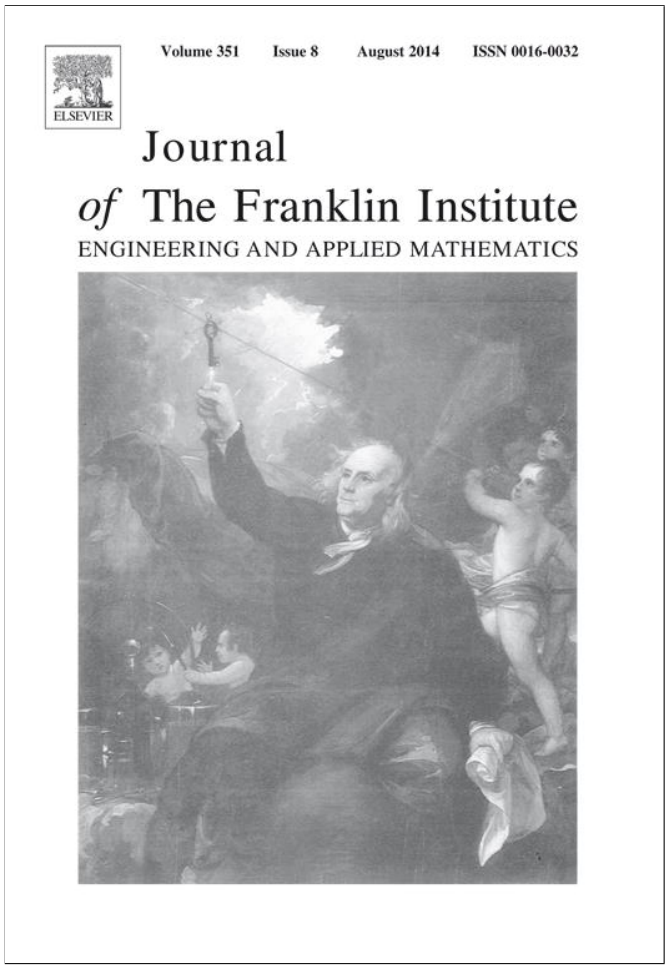

Available online at www.sciencedirect.com

ScienceDirect

Journal of the Franklin Institute 351 (2014) 4183–4197

Journal of The Franklin Institute

www.elsevier.com/locate/jfranklin

Model uncertainty estimation of a solid oxide fuel cell using a Volterra-type model

S.I. Biagiola*, C. Schmidt, J.L. Figueroa

Instituto de Investigaciones en Ingeniería Eléctrica (UNS – CONICET), Avda. Alem 1253, 8000 Bahía Blanca, Argentina

Received 12 November 2013; received in revised form 18 February 2014; accepted 25 April 2014
Available online 13 May 2014

Abstract

The dynamic nature of solid oxide fuel cells (SOFC) shows that they can be conceived as multi-input multi-output nonlinear processes. Aiming at dynamic simulation and control, this work presents a modeling study of a SOFC stack following a gray-box modeling approach. For such purpose, a Modified Generalized Memory Polynomial (MGMP) model is identified based only on input–output data of the system. Additionally, dedicated estimation is dealt with in order to cope with the presence of possible model uncertainty. Simulation results are given to illustrate the quality of the obtained model which is compared with other modeling approaches.

1. Introduction

Increasing demands on pollution reduction and stringent environmental regulations restricting emissions have narrowed down the search for a clean source of energy to a few options. Among these options, fuel cells are regarded as one of the most promising technologies, due to their efficiency, flexibility in sizing, quiet operation and reliability.

Fuel cells produce direct current electricity avoiding the conventional combustion reaction. In this way, fuel cells promise to emerge as feasible alternative to decrease fossil combustible

*Corresponding author at: Departamento de Ingeniería Eléctrica y de Computadoras, U.N.S., Avda.Alem 1253, (8000) Bahía Blanca, Argentina. Tel.: +54 291 4595101x3338; fax: +54 291 4595154.
E-mail address: biagiola@uns.edu.ar (S.I. Biagiola).

http://dx.doi.org/10.1016/j.jfranklin.2014.04.025

dependence. Therefore, based on their advantageous qualities, fuel cells are a desirable source of power generation for a broad range of applications and markets [1].

Their most common application is in large, stationary power plants. As they operate at high temperatures, "co-generation" is allowed [2]. This means that waste heat can be harnessed to generate steam for different applications such as heating, industrial processing, as well as steam turbines to produce additional electricity [3].

Mathematical models of SOFC are useful tools for both understanding and analyzing effects of diverse design and operation parameters on fuel cell performances. Moreover, important tasks such as designs optimization and selection of optimal conditions for operation can be supported on modeling results and simulation [4].

Due to the operation conditions, durability and efficiency of SOFC can be considerably improved if optimal control is implemented. In order to develop control algorithms for SOFC, it is necessary to understand their dynamic behavior [5]. This fact has prompted research activities in the field of SOFC to dedicated control strategies [4,6–10].

In the past years there has been an intensive search for models that represent the dynamical behavior of SOFC. These numerous attempts yielded many fruitful results on mathematical modeling of these fuel cells [4,10].

Many different types of models have been presented for SOFC. In one extreme there are those representation known as "white-box" models, which are based on first principles [11]. These approaches are oriented to physical phenomena that take place inside the cell, such as mass, electrical and thermal transports. Different factors that give rise to energy losses are included as well. Among the works that followed this *white-box* modeling strategy, the detailed reports provided by Spivey et al. [12,10] can be mentioned. In [13] fundamental relations that govern a fuel cell operation were utilized in both a lumped and a distributed modeling approach proposals. A detailed modeling approach was followed in [14], in which the developed model consists of mass, momentum and charge conservation equations, relating gas concentration to voltage, current density, and other relevant fuel cell parameters. The state-of-the-art of the SOFC modeling efforts and perspective on the subject were reported in [15,16,4].

On the other hand, *gray-box* and *black-box* models developed for SOFC can be mentioned. These approaches do not care about intrinsic phenomena that take place inside the cell. In a black-box model there is no a priori information available, only input–output data from the process are used to perform the model identification [17–19]. To develop effective control strategies, Jurado [20] presented an autoregressive with exogenous input (ARX) identification model for the SOFC. A *gray-box* model is one that has a known structure (generally constrained to a strict subset of the class of models it is drawn from) but has unknown parameters [21,22]. Many works concerned with this modeling approach have been dedicated to SOFC. To obtain an improved description of the nonlinear dynamics associated to the SOFC stack, Hammerstein models were developed by Jurado [23] and Huo et al. [8]. These models are special kinds of nonlinear systems in which a static nonlinear block is followed by a linear dynamic system [24]. This type of descriptions allows to overcome some of the typical limitations of linear models to represent nonlinear dynamics.

The aim of the present work is to develop a control-oriented dynamic model of SOFC stack. Such model must be able to predict the state variables and the performance of the solid oxide fuel cell. A discrete-time Volterra model (DTVM) is proposed for this purpose.

Several appealing versions of the DTVM have emerged in the context of compensation of nonlinear systems [25,26]. Simplicity and generalization are its two outstanding properties. In particular, the Modified Generalized Memory Polynomial (MGMP) model allows the

representation of a much more complex type of systems than simple Hammerstein and Wiener models (defined as in [27]). Based only on a set of input–output data from the system, the parameterized MGMP model can be identified. Moreover, any available information about the time constants of the process can be easily integrated to the model. In such a way, an efficient parameter model for real-time emulation and control of a SOFC is developed.

Once the first goal is achieved, i.e. the identification of MGMP model for nominal conditions, an important improvement is to perform robust identification to cope with the presence of uncertainty. That is the additional contribution of the present work, which deals with the formulation of the uncertainty as a set of parameters bounds which are found through the solution of an optimization problem. The methodological approach is based on the assumption that an uncertain parametric block oriented model must be identified. Moreover, the source of such uncertainty is assumed unknown. The resulting identification procedure is robust in the sense that the identified set of parameters is such that any of the collected data can be reproduced by at least one of the models in the set.

The work is organized as follows. In Section 2 general principles of SOFC are explained. In Section 3 the multivariable input–single output MGMP model is introduced and the associated identification problem is dealt with, while in Section 4 simulation results illustrating the performance of the proposed modeling algorithms on SOFC are presented. In Section 5, a procedure to characterize the parametric uncertainty in the model is described. Finally, conclusions and suggestion for future work are addressed in Section 6.

2. Fuel cell dynamics

A fuel cell is an energy conversion device that produces electricity from hydrogen and oxygen. The primary components of a fuel cell are an ion conducting electrolyte, an anode, and a cathode. Inside the cell, a voltage drop between electrodes is generated due to the catalytic oxidation of hydrogen in an anode and the catalytic reduction of oxygen in the cathode. Therefore, such voltage drop can be used by an external circuit if the electrolyte isolates both electrodes but allows ions mass and charge exchange.

When a fuel gas containing hydrogen flows over the anode, negatively charged oxygen ions move across the electrolyte to oxidize the fuel. An oxygen flow ($q^{in}_{O_2}$) is supplied, usually from air, at the cathode. Electrons generated at the anode move through an external load to the cathode, completing the circuit and supplying electric power.

The involved chemical reactions are described as

$$\begin{aligned} &\text{Anode side}: H_2 + O^{2^-} \rightarrow H_2O + 2e^- \\ &\text{Cathode side}: \tfrac{1}{2}O_2 + 2e^- \rightarrow O^{2^-} \\ &\text{Overall reaction}: \tfrac{1}{2}O_2 + H_2 \rightarrow H_2O \end{aligned} \tag{1}$$

The dynamic behavior of a SOFC is proposed in [28], where partial pressure calculation of the different species (H_2, O_2 and H_2O) is provided, as well as the resultant stack voltage (U) determination under the assumption of fluctuating load operation (i.e., variations in the current I).

It should be remarked that to guarantee the SOFC remains in a feasible operative region, a physical constraint between the inlet hydrogen flow and the current I should be satisfied. This restriction associated to hydrogen partial pressure has been modeled as $q^{in}_{H_2} \geq 2K_rI$ [23], where $q^{in}_{H_2}$ stands for the inlet hydrogen flow and K_r is a constant.

Multiple types of irreversible losses were taken into account in the SOFC dynamics simulation, which is an important issue because losses make the cell potential to diminish with respect to its ideal value. Though ohmic loss is the most cited one, activation and concentration losses may be mentioned as well. This more realistic situation in which all types of losses are present was considered in [7].

Note that it must be allowed that oxygen completely reacts with hydrogen. Moreover, the pressure difference between the anode and the cathode should be kept below a certain threshold value. Therefore, an oxygen surplus should be provided by means of using an appropriate hydrogen–oxygen flow ratio r_{H-O}.

The solid oxide fuel cell (SOFC) is viable for generating electricity from hydrocarbon fuels. Padullés et al. [28] assumed pure hydrogen as fuel source. However, if natural gas instead of hydrogen is used as fuel, the dynamics of the fuel processor must be included in the model ([28] and references therein). This more general approach was followed by Wu et al. [7], who modeled this behavior as a linear first order dynamics.

In this work, SOFC input–output data were generated to accomplish the proposed identification procedure. For such purpose, the model in [7] was arbitrarily selected for data generation, and the resultant cell samples were used to identify a MGMP model. Both nominal and uncertainty estimation approaches were performed.

It must be remarked that the identification approach herein presented is not tightened to any particular SOFC model, it only requires input–output data from the system.

3. The MGMP model

Lately, attractive variants of the discrete-time Volterra model (DTVM) have emerged mainly tied up to compensation of nonlinear systems [25,26]. DTVMs happen to be appealing mathematical representations due to their main properties: simplicity and generalization capability. Specifically, the Modified Generalized Memory Polynomial (MGMP) model allows the representation of a much more complex type of systems than simple (as defined in [27]) Hammerstein and Wiener ones. In its typical form, this model adopts the structure depicted in Fig. 1.

Provided that the structure is formed by an N-th order polynomial and a finite impulsive response (FIR) filter of order M, then the model output can be written as

$$\hat{y}(k) = \sum_{n=1}^{N} \left(\sum_{m=0}^{M-1} \alpha_{nm} u(k-m) \right)^{n} \tag{2}$$

where α_{nm} stands for the FIR filter parameters. Note that the model output is not linear in the model parameters and this fact could lead, in general, to a complex identification algorithm.

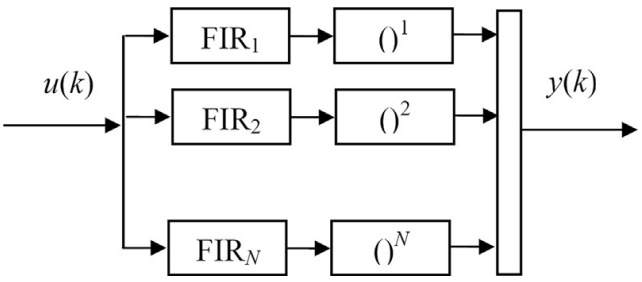

Fig. 1. General structure of a Modified Generalized Memory Polynomial model.

An important drawback of these models, which are based on FIR descriptions to represent dynamics behavior, is that they can demand an excessive amount of parameters to describe those systems whose impulse response decays slowly. To overcome this fact, we propose the use of linear filters which assimilate prior knowledge about the process dynamics in order to decrease the number of parameters. Specifically, the main underlying idea is to replace the tap delay used by the FIR filters (Fig. 1) by orthogonal bases [29,30]. In this way, the input sequence $\{u(k)\} \in \Re^{N_u}$ is mapped to a sequence of intermediate signals $\{z(k)\} \in \Re^{N_z}$, where $z(k)$ is the vector formed by signals

$$z_{j,p_{\{j\}}}(k) = B_{j,p_{\{j\}}}(q)u_j(k), \tag{3}$$

for $j = 1, \ldots, N_u$ and $p_{\{j\}} = 1, \ldots, N_{z\{j\}}$; where q is the forward time operator, $N_{z\{j\}}$ is the number of terms in the orthonormal basis from the jth input to the output,[1] u_j is the jth entry of the input vector and the $B_{j,p_{\{j\}}}(q)$ are the elements that relate the jth input to the output via the intermediate variables z. Therefore, the total number of subsystems is N_u.

The bases are defined as

$$B_{j,0}(q) = \frac{(1-\xi_j^2)^{1/2}}{q-\xi_j}, \tag{4}$$

and

$$B_{j,p_{\{j\}}}(q) = B_{j,(p_{\{j\}}-1)}(q)\left(\frac{1-\xi_j q}{q-\xi_j}\right), \quad p_{\{j\}} = 1, \ldots, N_{z\{j\}}. \tag{5}$$

Note that from this definition, the total number of internal variables is

$$N_z = \sum_{j=1}^{N_u} N_{z\{j\}}. \tag{6}$$

The proposed model allows to use the previous knowledge about the dominant modes of any of the subsystems from each input to each output. In this way, the knowledge about each mode can be incorporated to the model as parameters ξ_j.

Based on the previous description in terms of the bases elements, $z(k) \in \Re^{N_z}$ is mapped to the output $y(k) \in \Re$, through the following model output expression:

$$\hat{y}(k) = \sum_{n=1}^{N} (\boldsymbol{\alpha}_n^T \; v(k))^n, \tag{7}$$

where $v(k) = [z^T(k) \; u^T(k)]^T$ and $\boldsymbol{\alpha}_n \in \Re^{N_z+N_u}$ is the parameter vector related to the nth power term. Note that, in this representation, the direct influence of the input $u(k)$ on the output $y(k)$ is allowed.

From Eq. (7), it is clear that the output is not linear in the parameters. Therefore, it is not possible to use the classical LS solution. To overcome this difficulty, the proposal is to solve the LS problem using an optimization program. The approximation error for the output at time k is given as

$$e(k) = y(k) - \sum_{n=1}^{N} (\boldsymbol{\alpha}_n^T \; v(k))^n, \tag{8}$$

[1] Since that this application is a MISO system, this description is reduced to a single output

and the identification could be performed by solving the following problem:

$$\hat{\boldsymbol{\alpha}} = \arg\min_{\boldsymbol{\alpha}} \sum_{k=1}^{K} (e(k))^2 \tag{9}$$

where $\boldsymbol{\alpha} = [\boldsymbol{\alpha}_1, \ldots, \boldsymbol{\alpha}_N] \in \Re^{(N_z+N_u)N}$. Note that this involves an unconstrained nonlinear optimization problem. In order to improve the convergence of this identification algorithm, the analytical expressions of both gradient and Hessian are provided (see the Appendix).

In the following section numerical results are obtained to show the validation and approximation properties of the proposed MGMP structure for modeling a SOFC.

4. Identification of a fuel cell plant

In the context of system identification, and provided the dynamics description given in Section 2 for the SOFC, the model inputs are the current I and the fuel flowrate q_f (i.e. $u = [I\ q_f]^T$). On the other hand, the output is the voltage, i.e. $y = [U]$. Therefore, we deal with a two-input one-output process for the identification.

The nominal value considered for the current was 350 A and for the fuel flowrate was 0.8×10^{-3} kmol/s.

In a first step, simulation of the nonlinear model was performed to collect the necessary input–output data of this nonlinear process. For such purpose, random step changes with uniformly distributed amplitude were applied to the inputs I and q_f. A sample time of 5 s was assumed and each input was maintained constant for 120 samples before the next change took place. In order to obtain a persistent excitation, the input changes were not introduced simultaneously, i.e. I and q_f changed alternately. This means that when the value of I changed, it had been previously held for 120 samples while the value of the other input (i.e., q_f) had been held for 60 samples. The same commutation pattern was applied for changes in q_f.

The amplitude of the changes considered for the inputs were in the interval of ± 30 A and $\pm 1 \times 10^{-5}$ kmol/s around the nominal values of I and q_f, respectively, but subject to the physical constraint between the inlet hydrogen flow and the current, as mentioned in Section 2.

A total amount of 120,000 samples were obtained, half of them were used for model approximation and the rest for the validation test. A portion of the input signals sequences used for SOFC excitation are depicted in Fig. 2.

The dominant poles in the Laguerre basis were chosen taking into account a preliminary linear identification for an ARX model. For each input three poles are used ($\xi_1 = 0.9671, \xi_2 = 0.8211$ and $\xi_3 = -0.0272$). Second order expansions were selected for each input. In this form, the dimension of the vector $v(k)(k)$ is 14 (i.e., two entries for each pole and for each input, plus one entry for each input). A third order nonlinearity was chosen, i.e. $N=3$.

Before performing the identification, the three signals involved (U, q_f and I) were normalized to the range $[-1, 1]$. In order to compare the proposed model with other mathematical representations found in the literature for SOFC, the following models were considered:

- *A linear model*: This consists in the Laguerre optimal approximation (using all the poles for each input as described above).

  Then, the linear model of order N_l is represented by

$$y(k) = \mathcal{L}u(k), \tag{10}$$

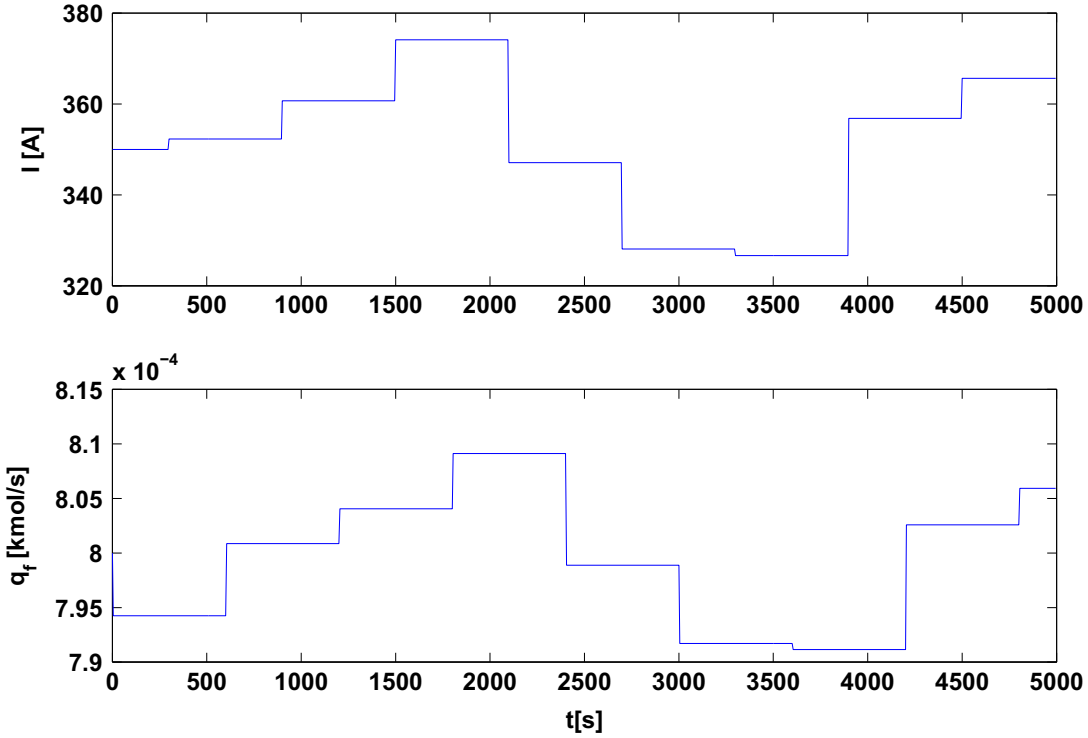

Fig. 2. Input sequences used for identification.

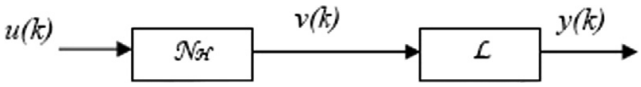

Fig. 3. Hammerstein model.

with

$$\mathcal{L}(q) = \sum_{i=0}^{N_l} h_i L_i(q,a) \tag{11}$$

$$L_i(q,a) = \frac{\sqrt{1-a^2}}{q-a}\left(\frac{1-aq}{q-a}\right)^i \tag{12}$$

where the parameters of the model are the coefficients h_i, the functions $L_i(q,a)$ are the Laguerre basis for LTI models and $a \in \Re$, with $|a|<1$, is a filter coefficient chosen a priori [22,30].

- *A Hammerstein model*: Its structure is depicted in Fig. 3.
  The nonlinear part of the model is represented as

$$v(k) = \mathcal{N}_H(u(k)) = \sum_{i=1}^{N_n} p_i g_i(u(k)), \tag{13}$$

where $g_i(\cdot)$ are the orthogonal bases and p_i are the unknown parameters of the nonlinear block which must be determined [31]. Here, we considered the nonlinear block is modeled as a third order polynomial, and the linear block is represented by a Laguerre approximation (as in Eqs. (11) and (12). As this model is used exclusively for comparison purposes, only step 1 of the identification is performed (i.e. the obtained model is overparameterized).

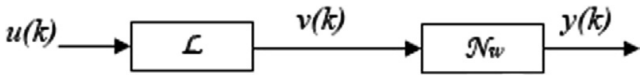

Fig. 4. Wiener model.

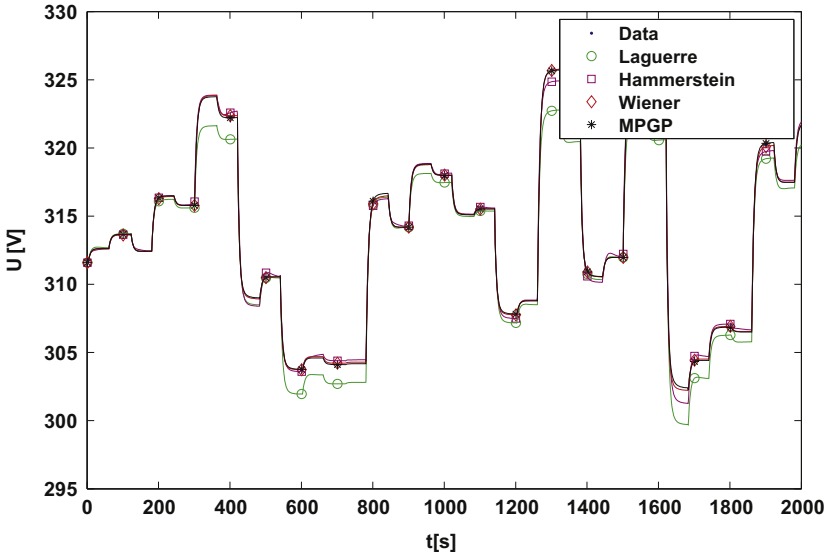

Fig. 5. Approximation results: process data vs. models outputs.

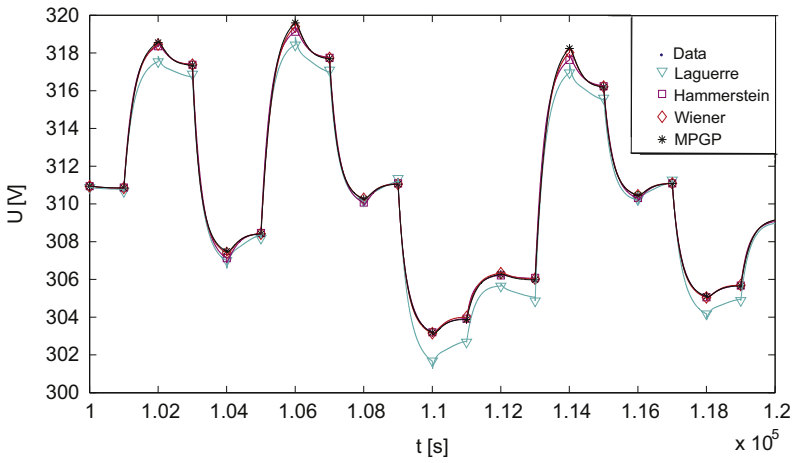

Fig. 6. Validation results: process data vs. models outputs.

- *A Wiener model*: As shown in Fig. 4 it is built up with the same blocks than the Hammerstein model but connected in the reverse order [31].
- *The proposed MPGP model*: This is obtained by solving the optimization problem described in Eq. (9). The resulting parameters $\hat{\boldsymbol{\alpha}}$ will be referred to as *nominal* ones in what follows.

Figs. 5 and 6 show the process data as well as the output predictions, for approximation and validation, respectively. In order to provide a reasonable measure to state a comparison between these models, the Root Mean Squares Error between the actual and the predicted outputs was considered. Table 1 shows the prediction results obtained for the whole set of data used for approximation and validation. The fourth column in Table 1 gives information about the number of parameters required by each model to achieve such performance. Simulation results show that the MPGP model yields higher modeling accuracy than the other ones.

Table 1
Approximation and validation errors.

Model	Approximation	Validation	Parameters
Laguerre	264.97	274.87	14
Hammerstein	87.80	91.54	42
Wiener	20.49	20.32	16
MPGP	8.39	9.85	42

Another important quality of the Volterra-like model is that it can reproduce extreme SOFC dynamics, i.e. both the faster and slower modes. This fact obeys to the coexistence of electrical, mass and thermal transports that evidence quite different time behavior [10].

5. Uncertainty characterization

In this section, the uncertainty related with MPGP model will be characterized. In particular, a robust identification procedure for this model will be presented and, afterwards, it will be applied to the SOFC data. The robust algorithm can be interpreted as an *extension* of the nominal MPGP model dealt with in the previous section, i.e. we are interested in quantifying the uncertainty related with the nominal model. In this way, we follow the typical *parameter intervals approach* which consists in defining a set of possible models to represent all the observed process behaviors [32,33]. This identification procedure is accomplished considering a set of parameters $\boldsymbol{\alpha}$ (with $\boldsymbol{\alpha} \in \Theta$) such that when these parameters $\boldsymbol{\alpha}$ are used, the whole set of input sequences $\mathbf{u}$ is "mapped" onto a predicted output set which contains the measured output data $\mathbf{y}$. Therefore, the proposed identification method assumes an uncertain set made up by many models with identical structure but different parameters. Such models' family is defined using a parametric approach as follows:

$$\Theta = \{\boldsymbol{\alpha} : \boldsymbol{\alpha} = \hat{\boldsymbol{\alpha}} + \Delta\boldsymbol{\alpha};\ -\Delta\boldsymbol{\alpha}_L \le \Delta\boldsymbol{\alpha} \le \Delta\boldsymbol{\alpha}_U\}. \tag{14}$$

where the estimated parameter $\hat{\boldsymbol{\alpha}}$ is obtained by means of Eq. (9). The symbol $\boldsymbol{\alpha}$ stands for the actual (unknown) model parameter vector, and $\Delta\boldsymbol{\alpha}$ is a bounded increment. In order to describe the uncertainty, the parameter bounds $\Delta\boldsymbol{\alpha}_L$ and $\Delta\boldsymbol{\alpha}_U$ (with $\Delta\boldsymbol{\alpha}_L \in \Re^+$ and $\Delta\boldsymbol{\alpha}_U \in \Re^+$) should be computed in such a way that at any time $k = 1, \ldots, K$ and for any input $u(k)$ the output of the system $y(k)$ lies in the set

$$Y = \left\{ \hat{y}(k) : \hat{y}(k) = \sum_{n=1}^{N} (\boldsymbol{\alpha}_n^T\ v(k))^n;\ \forall \boldsymbol{\alpha} \in \Theta \right\}. \tag{15}$$

This identification approach can be written as an optimization problem

$$\min_{\Delta\boldsymbol{\alpha}_L, \Delta\boldsymbol{\alpha}_U} \| \Delta\boldsymbol{\alpha}_L + \Delta\boldsymbol{\alpha}_U \| \tag{16}$$

subject to

$$\max_{\Delta\boldsymbol{\alpha} \in [\Delta\boldsymbol{\alpha}_L, \Delta\boldsymbol{\alpha}_U]} \sum_{n=1}^{N} (\boldsymbol{\alpha}_n^T\ v(k))^n \ge y(k) \quad \text{for all } k = 1, \ldots, K \tag{17}$$

$$\min_{\Delta\boldsymbol{\alpha} \in [\Delta\boldsymbol{\alpha}_L, \Delta\boldsymbol{\alpha}_U]} \sum_{n=1}^{N} (\boldsymbol{\alpha}_n^T\ v(k))^n \le y(k) \quad \text{for all } k = 1, \ldots, K. \tag{18}$$

The solution to this problem is complex due to the presence of the 2 K constraints involved in the optimization. In order to reduce this complexity, in the following we develop an ad hoc strategy to work out, in a very efficient way, the problem associated to such constraints.

Since the entries of the vector $v(k)$ could be positive or negative, it is possible to split it into two, by defining $v^+(k) = \max(v(k), 0)$ and $v^-(k) = \min(v(k), 0)$. Then, we can write

$$\max_{\Delta\boldsymbol{\alpha} \in [\Delta\boldsymbol{\alpha}_L, \Delta\boldsymbol{\alpha}_U]} (\boldsymbol{\alpha}_n^T \ v(k)) = (\hat{\boldsymbol{\alpha}}_n - \Delta\boldsymbol{\alpha}_L)^T v^-(k) + (\hat{\boldsymbol{\alpha}}_n + \Delta\boldsymbol{\alpha}_U)^T v^+(k) \triangleq (\gamma_U)_n \tag{19}$$

and

$$\min_{\Delta\boldsymbol{\alpha} \in [\Delta\boldsymbol{\alpha}_L, \Delta\boldsymbol{\alpha}_U]} (\boldsymbol{\alpha}_n^T \ v(k)) = (\hat{\boldsymbol{\alpha}}_n + \Delta\boldsymbol{\alpha}_U)^T v^-(k) + (\hat{\boldsymbol{\alpha}}_n - \Delta\boldsymbol{\alpha}_L)^T v^+(k) \triangleq (\gamma_L)_n. \tag{20}$$

Based on these definitions, the solution of the maximization problem stated in (17) is

$$\max_{\Delta\boldsymbol{\alpha} \in [\Delta\boldsymbol{\alpha}_L, \Delta\boldsymbol{\alpha}_U]} \sum_{n=1}^{N} (\boldsymbol{\alpha}_n^T \ v(k))^n = \sum_{n_{odd}=1}^{N} \left((\gamma_U)_{n_{odd}}\right)^{n_{odd}} + \sum_{n_{even}=2}^{N} \max\left\{ \left((\gamma_L)_{n_{even}}\right)^{n_{even}}, \left((\gamma_U)_{n_{even}}\right)^{n_{even}} \right\} \triangleq \Gamma_U \tag{21}$$

where $n_{odd} \in \aleph$ and $n_{odd} \in \aleph$ stand for odd and even numbers, respectively. Analogously, the solution of the minimization problem in Eq. (18) is

$$\min_{\Delta\boldsymbol{\alpha} \in [\Delta\boldsymbol{\alpha}_L, \Delta\boldsymbol{\alpha}_U]} \sum_{n=1}^{N} (\boldsymbol{\alpha}_n^T \ v(k))^n = \sum_{n_{odd}=1}^{N} \left((\gamma_L)_{n_{odd}}\right)^{n_{odd}} + \sum_{n_{even}=2}^{N} \min\left\{ \left((\gamma_L)_{n_{even}}\right)^{n_{even}}, \left((\gamma_U)_{n_{even}}\right)^{n_{even}} \right\} \triangleq \Gamma_L. \tag{22}$$

Therefore, the problem of the uncertainty characterization in Eq. (16) could be formulated as follows:

$$\min_{\Delta\boldsymbol{\alpha}_L, \Delta\boldsymbol{\alpha}_U} \| \Delta\boldsymbol{\alpha}_L + \Delta\boldsymbol{\alpha}_U \| \tag{23}$$

subject to

$$\sum_{n_{odd}=1}^{N} \left((\gamma_U)_{n_{odd}}\right)^{n_{odd}} + \sum_{n_{even}=2}^{N} \max\left\{ \left((\gamma_L)_{n_{even}}\right)^{n_{even}}, \left((\gamma_U)_{n_{even}}\right)^{n_{even}} \right\} \geq y(k), \tag{24}$$

$$\sum_{n_{odd}=1}^{N} \left((\gamma_L)_{n_{odd}}\right)^{n_{odd}} + \sum_{n_{even}=2}^{N} \min\left\{ \left((\gamma_L)_{n_{even}}\right)^{n_{even}}, \left((\gamma_U)_{n_{even}}\right)^{n_{even}} \right\} \leq y(k). \tag{25}$$

The parametric uncertainty is computed by solving this optimization problem for the whole set of measured input–output data.

The identification algorithm was efficiently performed on a 2.13 GHz Intel Core I3 processor using MATLAB 7.8.0 optimization Toolbox. For the nominal model "fminunc" routine was used with explicitly calculated gradient and Hessian. As regards the uncertainty characterization "fmincon" routine was performed. In this case, the same options for gradient and Hessian were considered in the objective function, but leaving the gradients of the constraints in default mode (i.e. numeric calculation was accomplished).

The calculated nominal parameters (NP) and their lower and upper bounds (LB and UB, respectively) are detailed in Table 2. Note that the identified parameter α_1 (together with its bounds) allows describing the uncertainty appropriately.

Table 2
Estimation results.

$\alpha_1 \times 10^{-4}$			$\alpha_2 \times 10^{-3}$			$\alpha_3 \times 10^{-4}$		
LB	NP	UB	LB	NP	UB	LB	NP	UB
−0.0004	0.0011	0.0011	−0.0377	−0.0377	−0.0377	−0.1416	−0.1416	−0.1416
−0.0003	−0.0003	−0.0003	0.0109	0.0109	0.0109	0.0417	0.0417	0.0417
0.0036	0.0036	0.0036	−0.0580	−0.0580	−0.0580	−0.2910	−0.2910	−0.2910
−0.0025	−0.0025	−0.0025	0.0595	0.0595	0.0595	0.255	0.255	0.255
0.0012	0.0012	0.0012	−0.0001	−0.0001	−0.0001	−0.8798	−0.8798	−0.8798
0.0041	0.0041	0.0041	−0.0551	−0.0551	−0.0551	−0.5386	−0.5386	−0.5386
−3.4181	−3.4163	−3.4163	−5.8182	−5.8182	−5.8182	−0.3978	−0.3978	−0.3978
−0.0440	−0.0402	−0.0274	0.0099	0.0099	0.0099	0.238	0.238	0.238
2.3322	2.3322	2.3337	2.5216	2.5216	2.5216	−1.0959	−1.0959	−1.0959
−0.0419	−0.0433	−0.0433	0.2597	0.2597	0.2597	0.6683	0.6683	0.6683
−0.0132	−0.0132	−0.0132	0.2553	0.2553	0.2553	1.1353	1.1353	1.1353
−0.0114	−0.0114	−0.0114	0.1841	0.1841	0.1841	1.0049	1.0049	1.0049
0.0153	0.0153	0.0153	−0.3130	−0.3130	−0.3130	−1.1312	−1.1312	−1.1312
−0.0004	−0.0004	−0.0000	0.0083	0.0083	0.0083	0.0404	0.0404	0.0404

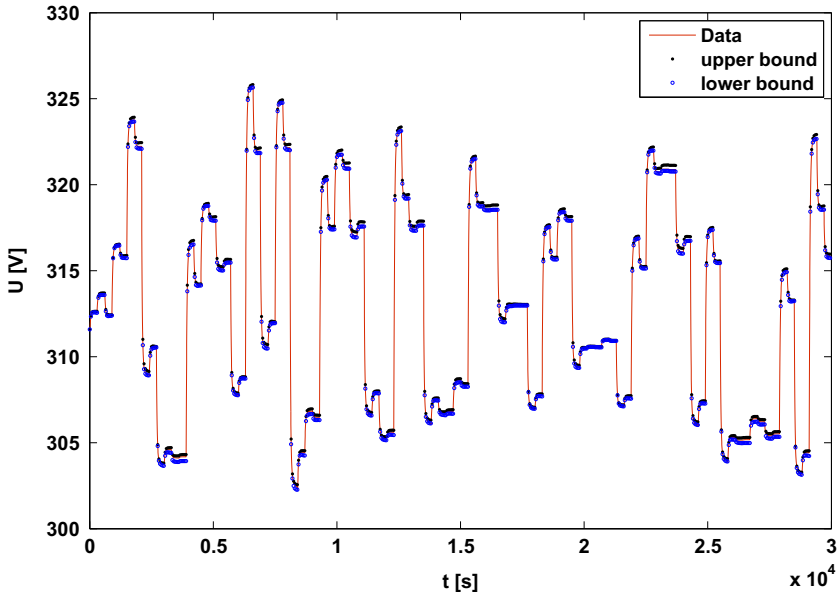

Fig. 7. Uncertainty bounds for MPGP model.

Fig. 7 shows the calculated bounds for a portion of the collected data. From Fig. 7 it can be observed the collected output data of the process are between the bounds determined through robust identification. It is important to highlight the tight bounds obtained with this modeling approach. These results can be compared with the ones obtained with the uncertain Laguerre model (Fig. 8), which are computed using the procedure described in [34]. Note that in this case (i.e., the uncertain Laguerre model) the calculated bounds are significantly more conservative.

It should be considered the fact that the measured output could be corrupted with noise. This more realistic situation, common in practice, could be easily included in the present identification

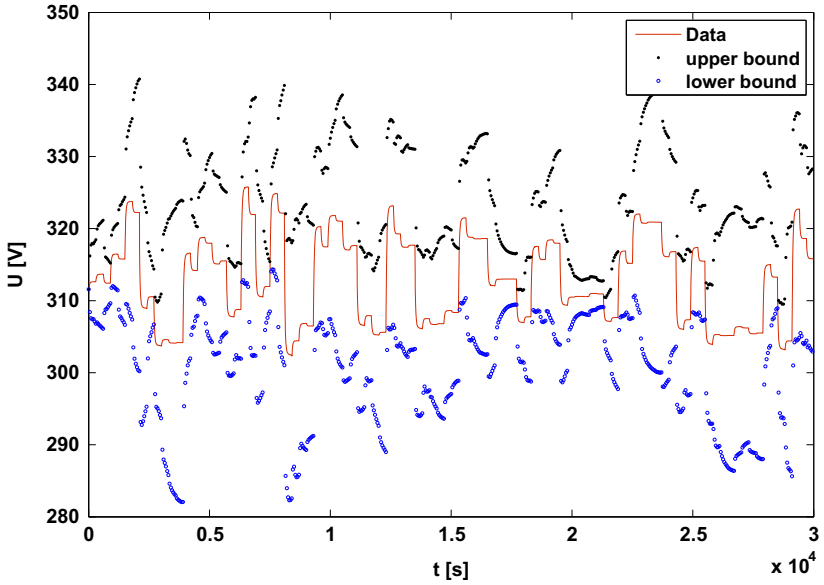

Fig. 8. Uncertainty bounds for Laguerre model.

approach. Data acquisition can involve different noise sources, the inclusion of such measurements in Eqs. (17) and (18) would lead to artificially increased uncertainty on the parameter bounds. Provided the measured output is $y(k)+e(k)$, and that the additive noise $e(k)$ is such that $|e(k)| \leq \epsilon \in \Re^+$, then

$$\max_{\Delta\boldsymbol{\alpha} \in [\Delta\boldsymbol{\alpha}_L, \Delta\boldsymbol{\alpha}_U]} \sum_{n=1}^{N} (\boldsymbol{\alpha}_n^T \; v(k))^n \geq y(k) + \epsilon \quad \text{for all } k = 1, \ldots, K \tag{26}$$

$$\min_{\Delta\boldsymbol{\alpha} \in [\Delta\boldsymbol{\alpha}_L, \Delta\boldsymbol{\alpha}_U]} \sum_{n=1}^{N} (\boldsymbol{\alpha}_n^T \; v(k))^n \leq y(k) - \epsilon \quad \text{for all } k = 1, \ldots, K. \tag{27}$$

Therefore, the identified uncertain model would be accounting for noisy measurements, and the conservativeness would be unnecessarily increased. Otherwise, it is possible to reduce the conservativeness if we replace the previous constraints by the following ones:

$$\max_{\Delta\boldsymbol{\alpha} \in [\Delta\boldsymbol{\alpha}_L, \Delta\boldsymbol{\alpha}_U]} \sum_{n=1}^{N} (\boldsymbol{\alpha}_n^T \; v(k))^n \geq y(k) - \epsilon \quad \text{for all } k = 1, \ldots, K \tag{28}$$

$$\min_{\Delta\boldsymbol{\alpha} \in [\Delta\boldsymbol{\alpha}_L, \Delta\boldsymbol{\alpha}_U]} \sum_{n=1}^{N} (\boldsymbol{\alpha}_n^T \; v(k))^n \leq y(k) + \epsilon \quad \text{for all } k = 1, \ldots, K. \tag{29}$$

This modification in the optimization algorithm allows including the known bounds of the measurement noise in order to reduce the estimated bounds of the model parameters. Note that inclusion of Eqs. (28) and (29) (instead of Eqs. (26) and (27)) could provoke the model's output prediction that differs from the measured output as much as ϵ. It is assumed that this possible bias is due to the noise and, under this hypothesis, it is no longer possible to guarantee that the sampled data will be completely justified by the model.

6. Conclusions

A dedicated approach for identification of SOFC stack was presented. The nonlinear model consists in a dynamic linear block, which can be represented by a finite set of discrete Laguerre or Kautz transfer functions, followed by a nonlinear static part which is a modification of a Volterra-like model (i.e., MGMP model).

The validity of the proposed model is evaluated by comparing its output prediction with the system output. Good agreement between both signals is achieved. Moreover, the proposed model prediction outperforms other models' predictions. This is a promising result, because linear models (e.g. ARX) and Hammerstein descriptions have been previously used for modeling SOFC.

A noniterative algorithm was also developed to perform uncertainty characterization for the proposed MISO MGMP model. Simulation results have illustrated the applicability of the proposed Volterra-like representation in modeling the nonlinear dynamic properties of the SOFC including an uncertainty parametric description. The model identification is only based on input–output data from the process, i.e. no further information about the internal SOFC dynamics is demanded.

Based on the attractive model approximation capacity and flexibility achieved with the proposed MGMP model, and provided the good description obtained for the uncertainty this model, the next step could be the design of a suitable MGMP model-based control structure to achieve robust control of SOFCs processes. This is a topic worthy of future research.

Acknowledgments

The authors gratefully acknowledge the financial support of Agencia Nacional de Promoción Científica y Tecnológica (PICT-2010-1421), CONICET (PIP 112-201101-01005) and Universidad Nacional del Sur.

Appendix

To improve the convergence of the optimization problem, the computation of both gradient and Hessian analytical expressions is accomplished. The objective function of the problem is

$$f(\boldsymbol{\alpha}) = \sum_{t=1}^{K} \left(y(t) - \sum_{n=1}^{N} (\boldsymbol{\alpha}_n^T \, v(t))^n \right)^2. \tag{30}$$

The gradient of $f(\boldsymbol{\alpha})$ with respect to the entries of $\boldsymbol{\alpha}$ is

$$\frac{\partial f(\boldsymbol{\alpha})}{\partial \boldsymbol{\alpha}_n} = -2n \sum_{t=1}^{K} e(t)(\boldsymbol{\alpha}_n^T \, v(t))^{n-1} v(t), \tag{31}$$

and the Hessian is

$$\frac{\partial^2 f(\boldsymbol{\alpha})}{\partial \boldsymbol{\alpha}_n \partial \boldsymbol{\alpha}_m} = -2n \sum_{t=1}^{K} \left(-m(\boldsymbol{\alpha}_m^T \, v(t))^{m-1} (\boldsymbol{\alpha}_n^T \, v(t))^{n-1} v^2(t) + \psi(n-1) e(t) (\boldsymbol{\alpha}_n^T \, v(t))^{n-2} v^2(t) \right) \tag{32}$$

where $\psi = 1$ only if $m = n$; otherwise $\psi = 0$.

References

[1] C. Kunusch, P.F. Puleston, M.A. Mayosky, Sliding Mode Control of PEM fuel cells, Springer, London, 2012.
[2] R. Barrera, S. De Biase, S. Ginocchio, S. Bedogni, L. Montelatici, Performance and life time test on a 5 kW SOFC system for distributed cogeneration, Int. J. Hydrog. Energy 33 (12) (2008) 3193–3196.
[3] M. Bavarian, M. Soroush, I.G. Kevrekidis, J.B. Benziger, Mathematical modeling, steady-state and dynamic behavior, and control of fuel cells: a review, Ind. Eng. Chem. Res. 49 (2010) 7922–7950.
[4] M. Murshed, B. Huang, Y. Qi, Solid oxide fuel cell: perspective of dynamic modeling and control, J. Process Control 21 (10) (2011) 1426–1437.
[5] D.J. Hall, R.G. Colclaser, Transient modeling and simulation of a tubular solid oxide fuel cell, IEEE Trans. Energy Convers. 14 (3) (1999) 749–753.
[6] Y.H. Li, S. Rajakaruna, S.S. Choi, Control of a solid oxide fuel cell power plant in a grid-connected system, IEEE Trans. Energy Convers. 22 (2) (2007) 405–413.
[7] X. Wu, X. Zhu, G. Cao, H. Tu, Predictive control of SOFC based on GA-RBF neural network model, J. Power Sources 179 (2008) 232–239.
[8] H. Huo, Z. Zhong, X. Zhu, H. Tu, Nonlinear dynamic modeling for a SOFC stack by using a Hammerstein model, J. Power Sources 175 (2008) 441–446.
[9] H. Huo, X. Zhu, W. Hu, H. Tu, J. Li, J. Yang, Nonlinear model predictive control of SOFC based on a Hammerstein model, J. Power Sources 185 (2008) 338–344.
[10] B.J. Spivey, T.F. Edgar, Dynamic modeling, simulation, and MIMO predictive control of a tubular solid oxide fuel cell, J. Process Control 22 (8) (2012) 1502–1520.
[11] L. Ljung, T. Glad, Modeling of Dynamic Systems, Prentice-Hall Inc., Englewood Cliffs, NJ, 1994.
[12] B.J. Spivey, Dynamic modeling, model-based control, and optimization of solid oxide fuel cells (Ph.D. thesis), The University of Texas at Austin, USA, 2011.
[13] A. Gebregergis, P. Pillay, D. Bhattacharyya, R. Rengaswemy, Solid oxide fuel cell modeling, IEEE Trans. Ind. Electron. 56 (1) (2009) 139–148.
[14] M. Angeloni, P. Lisbona, R. Bove, A PDE model for microscopic simulation of solid oxide fuel cells, J. Power Sources 201 (2012) 184–195.
[15] S. Kakaç, A. Pramuanjaroenkij, X. Zhou, A review of numerical modeling of solid oxide fuel cells, Int. J. Hydrog. Energy 32 (2007) 761–786.
[16] K. Wang, D. Hissel, M.C. Péra, N. Steiner, D. Marra, M. Sorrentino, C. Pianese, M. Monteverde, P. Cardone, J. Saarinen, A review on solid oxide fuel cell models, Int. J. Hydrog. Energy 36 (2011) 7212–7228.
[17] J. Sjöberg, Q. Zhang, L. Ljung, A. Benveniste, B. Delyon, P.Y. Glorennec, H. Hjalmarsson, A. Juditsky, Nonlinear black-box modeling in system identification: a unified overview, Automatica 12 (12) (1995) 1691–1724.
[18] A. Juditsky, H. Hjalmarsson, A. Benveniste, B. Delyon, L. Ljung, J. Sjöberg, Q. Zhang, Nonlinear black-box models in system identification: mathematical foundations, Automatica 31 (12) (1995) 1725–1750.
[19] J. Sjöberg, L.S.H. Ngia, Neural nets and related model structures for nonlinear system identifications, in: J.A. K. Suykens, J. Vandewalle (Eds.), Nonlinear Modeling: Advanced Black-Box Techniques, Kluwer Academic Publishers, Boston, 1998, pp. 1–27.
[20] F. Jurado, Modeling SOFC plants on the distribution system using identification algorithms, J. Power Sources 129 (2) (2004) 205–215.
[21] L. Ljung, System Identification: Theory for the User, Prentice-Hall Inc., Englewood Cliffs, NJ, 1999.
[22] O. Nelles, Nonlinear System Identification, Springer, Berlin, 2001.
[23] F. Jurado, A method for the identification of solid oxide fuel cells using a Hammerstein model, J. Power Sources 154 (2006) 145–152.
[24] A. Janczak, Identification of Nonlinear Systems Using Neural Networks and Polynomial Models, Springer, Berlin, 2005.
[25] F.J. Doyle III, R.K. Pearson, B. Ogunnaike, Identification and Control Using Volterra Models, Springer, London, Great Britain, 2002.
[26] D.R. Morgan, Z. Ma, J. Kim, M.G. Zierdt, J. Pastalan, A generalized memory polynomial model for digital predistortion of RF power amplifiers, IEEE Trans. Circuits Syst. 54 (10) (2006) 3852–3860.
[27] R. Haber, H. Unbenhauen, Structure identification of nonlinear dynamic system. A survey on input/output approaches, Automatica 26 (4) (1990) 651–677.
[28] J. Padullés, G.W. Ault, J.R. McDonald, An integrated SOFC plant dynamic model for power systems simulation, J. Power Sources 86 (2000) 495–500.

[29] B. Ninness, F. Gustafsson, A unifying construction of orthonormal bases for system identification, IEEE Trans. Autom. Control AC-42 (4) (1997) 515–521.
[30] J.C. Gómez, E. Baeyens, Identification of block-oriented nonlinear systems using orthonormal bases, J. Process Control 14 (6) (2004) 685–697.
[31] S.I. Biagiola, J.L. Figueroa, Identification of uncertain MIMO Wiener and Hammerstein models, Comput. Chem. Eng. 35 (2011) 2867–2875.
[32] P. Falugi, L. Giarré, G. Zappa, Approximation of the feasible parameter set in worst-case identification of Hammerstein models, Automatica 41 (6) (2005) 1017–1024.
[33] M.V. Kothare, V. Balakrishnan, M. Morari, Robust constrained model predictive control using linear matrix inequalities, Automatica 32 (1996) 1361–1379.
[34] J.L. Figueroa, S.I. Biagiola, M.P. Alvarez, L.R. Castro, O.E. Agamennoni, Robust model predictive control of a Wiener-like system, J. Frank. Inst. 350 (2013) 556–574.